High-Temperature Power Performance of X-Band Recessed-Gate AlGaN/GaN HEMTs

Cathy Lee, Paul Saunier, and Hua-Quen Tserng

TriQuint Semiconductor Texas, 500 W. Renner Rd. Richardson, TX 75080
E-mail: clee@tqtx.com

Abstract – Record power densities have been demonstrated with AlGaN/GaN HEMTs using the field-modulating plate gate structure. This approach creates a trade-off between breakdown voltage and gain, which can be improved by performing gate recessing. In this work, 0.25-µm recessed-gate AlGaN/GaN devices were fabricated on SiC. At 10 GHz, saturated power density of 6.35 W/mm with peak PAE of 50.2% with assoc. gain of 13.2 dB at peak PAE at V_{DS} = 35 V was achieved. Comparison of DC, small-signal, RF power, and high-temperature performance between recessed and non-recessed will be discussed.

Keywords – GaN, HEMT, Recess, High- Temperature

I. INTRODUCTION

Owing to its superior material properties, the AlGaN/GaN-based HEMTs have been recognized as the most promising devices for high-power applications at microwave and millimeter-wave frequency range. However, the power performance of the AlGaN/GaN-based devices has been limited by surface trap-induced current dispersion phenomenon, which reduces the RF current swing and increases the RF knee voltage under large-signal operation. Recently, the field-plated gate structure has been shown to effectively suppress the dispersion or current collapse effect and has significantly increased the gate-drain breakdown voltage. Record power densities have been demonstrated using this field-plate approach [1-2], however, one drawback of this approach is the additional feedback capacitance created by the over-lapping gate [1-2], resulting in the reduction of small-signal and large-signal gain. This trade-off between breakdown voltage and gain can be improved by recessing the gate and reducing the gate-to-channel distance. Several reports have shown improvements in transconductance and large-signal gain of recessed-gate devices with field-plate at 2 GHz [3-5]. There has been limited data on the power performance and gain improvements of recessed-gate devices with FP at X-band frequencies.

In this work, 0.25-µm recessed-gate AlGaN/GaN devices with field-plate were fabricated on SiC substrates. On the same wafer, non-recessed devices with the same field-plate length were also fabrication for direct comparison. At 10 GHz, saturated power density of 6.35 W/mm with peak PAE of 50.2% with assoc. gain of 13.2 dB at V_{DS} = 35 V was achieved on recessed-gate devices. The high gain achieved along with high PAE and power density at 10 GHz is a result of recess and field-plate structure. Comparison of DC and RF power performance of recessed devices to non-recessed devices will be shown. Power performance of large gate-periphery recessed devices will be discussed. In addition, the high temperature (up to 200 °C) power performance and the dependence of power and gate current on temperature for recessed-gate GaN devices will be reported.

II. DC AND SMALL SIGNAL RESULTS

The epitaxial layer consisted of a 10-Å GaN cap with 220 Å of AlGaN schottky barrier layer. After mesa isolation and ohmic contacts formation, silicon nitride was deposited to passivate the surface. The gate length was defined by etching a 0.25-µm window in the silicon nitride. On part the wafer, the gate recess was then performed using low-power RIE etching. Following the recess etch, the gate top and field-plate extensions were metalized on both the recessed and non-recessed devices, forming the field-plated gate.

0-7803-9250-7/05/$20.00 (c) 2005 IEEE

At V_{DS} = 10 V, the recessed-gate devices showed a 20% increase in maximum extrinsic transconductance, Gm,max, over the non-recessed devices. The average Gm,max of 50-µm recessed-gate devices were 279 mS/mm. The threshold voltage shifted from -4.2 V for non-recessed devices to -2.57 V as the devices were recessed with low-power RIE etching after nitride etch. Idss reduced from 830 mA/mm for the non-recessed devices to 680 mA as the AlGaN barrier layer was removed. Interestingly, the Idmax was nearly identical for both types of devices of 1 A/mm for the non-recessed devices and 950 mA/mm for the recessed devices. The 2-terminal breakdown voltage was changed significantly for the recessed structure, increasing the BV from 30 V to 63 V, which indicates that the SiNx-GaN interface could be a limiting factor for BV in our process. The small-signal performance was measured for both device types as a function of drain bias. At V_{DS} = 15 V, f_T was 35 GHz for both gate structures. F_T gradually decreased as the drain bias was increased. At V_{DS} = 35 V, the non-recessed devices exhibited f_T of 30 GHz, which is 3 – 4 GHz higher than the recessed devices. The equivalent circuit modeling shows the gate-source capacitance was higher for the recessed devices. Therefore, there were only slight differences in the f_T of the two types of devices.

III. RF POWER AND HIGH - TEMPERATURE RESULTS

The RF power performances of recessed and non-recessed FP devices were measured on-wafer at 10 GHz without any active cooling. Figure 1 compares the output power density at peak PAE as a function of V_{DS} of devices with gate width of 300-µm.

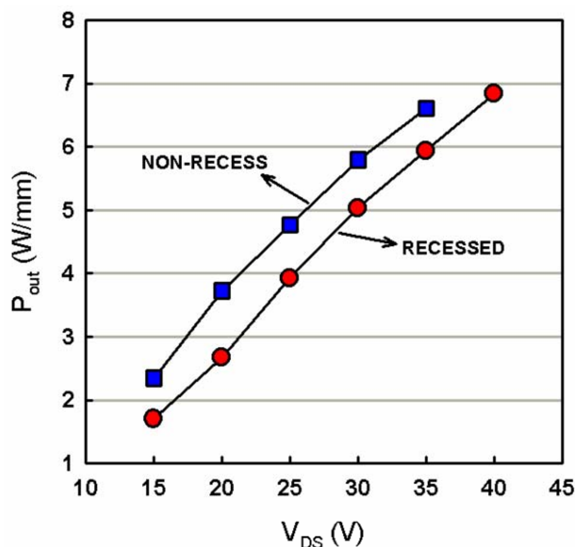

Figure 1. Output power density at peak PAE as a function of drain bias measured at 10 GHz of 300-µm recessed and non-recessed AlGaN/GaN HEMTs

The linear increase of Pout to V_{DS} for both recessed and non-recessed devices is a characteristic of devices with field-plate. At the same drain bias, the recessed devices showed an average reduction of 0.79 W/mm in Pout from the non-recessed counter parts. However, with the recessed devices, lower leakage current was observed both under DC and under RF drive, thus allowing the recessed devices to operate at higher drain voltage than the non-recessed devices. At 35 V, 6 W/mm of Pout with 50% PAE and 13 dB assoc. gain were achieved on the recessed-gate device. At 40 V, 7 W/mm of Pout was achieved with 12 dB gain. The peak PAE remained constant at 50 to 52 %from 15 V to 35 V for both recessed and non-recessed devices as shown in Fig. 2.

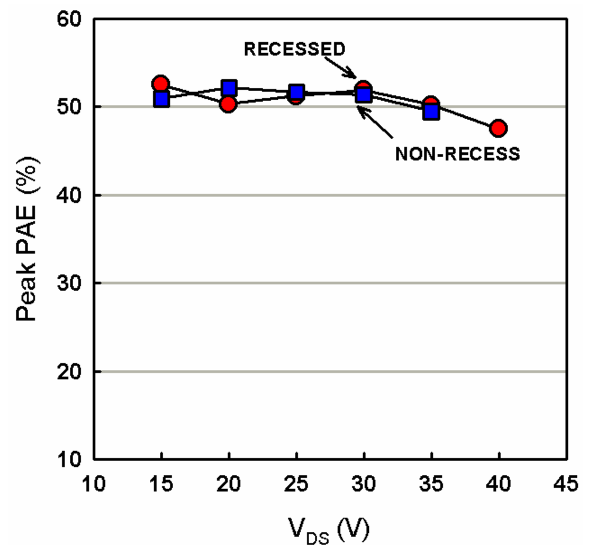

Fig. 2 Peak PAE as a function of drain bias measured at 10 GHz of 300-µm recessed and non-recessed AlGaN/GaN HEMTs

At 40 V, the non-recessed devices had excessive leakage current due to lower breakdown voltage, resulting in lower voltage of operation for the non-recessed devices.

Most importantly, Fig. 3 shows that the recessed devices exhibited an advantage of 3 dB in assoc. gain from 15 V to 35 V, and at 40 V, the recessed gate devices showed a linear gain of 16.8 dB with an assoc. gain of 12.9 dB at peak PAE. The linear gain of the recessed devices, as plotted in Figure 4, showed a similar increase of 3 – 4 dB at lower drain bias.

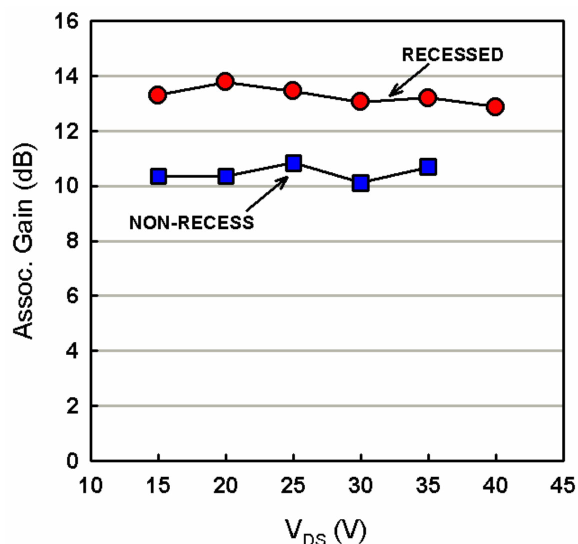

Fig. 3 Assoc. gain at peak PAE as a function of drain bias measured at 10 GHz of 300-µm recessed and non-recessed AlGaN/GaN HEMT

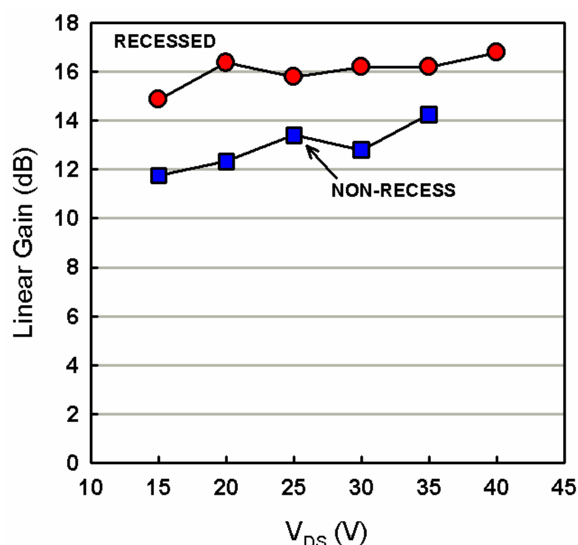

Figure 4. Linear gain as a function of drain bias measured at 10 GHz of 300-µm recessed and non-recessed AlGaN/GaN HEMT

A representative of the power sweep curves of a recessed-gate device with FP is shown in Fig. 5. At 35 V, high PAE and high gain were simultaneously achieved with the recessed-gate process.

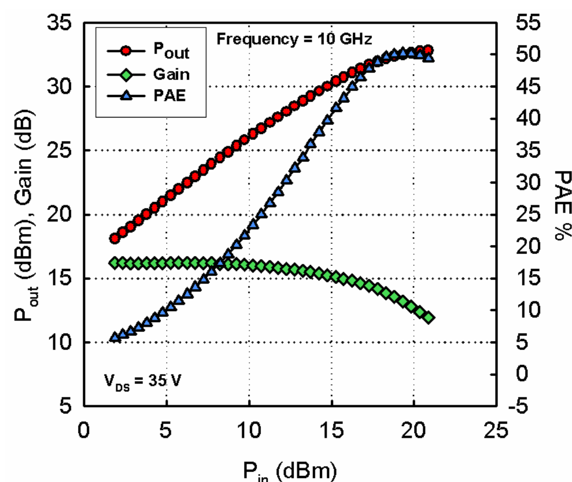

Fig. 5 Power sweep curves at Vds = 35 V of recessed AlGaN/GaN HEMTs

On a 1.5-mm recessed gate device, a saturated power of 7.2 W was achieved with peak PAE of 46% and power gain of 10 dB at V_{DS} = 40 V. Similar to the 300-µm devices, the peak PAE remained relatively constant at > 50% at V_{DS} = 15 V to 47 % at V_{DS} = 35 V. Another characteristic of the recessed gate devices was that the gate current remained low under RF drive, which allowed for higher voltage of operation.

The power performance of recessed-gate GaN devices with FP was characterized and compared with non-recessed devices as a function of temperature. The power was measured in every 25 °C from 25 °C to 200 °C. The initial output power density for non-recessed and recessed devices at V_{DS} = 25 V were 3.78 W/mm and 3.5 W/mm, respectively. The corresponding initial PAE and gain were 50% and 11.2 dB for non-recessed devices and 49.6% and 12.5 dB for recessed devices. Figure 6 shows that Pout of the recessed FP devices decreased at 0.014 dB/°C, which is similar to the non-recessed FP devices. At 200 °C, the non-recessed device showed higher power density of 2.55 W/mm compared with 2.2 W/mm of the recessed gate devices. On the other hand, the recessed devices still showed a significant advantage in associated gain at high temperature compared with the non-recessed devices. At 200 °C, an associated gain of 9.9 dB and 6.8 dB were measured for recessed devices and non-recessed devices, respectively. The difference is due to the increase in gate current at high temperature for the non-recessed devices as shown in Figure 7.

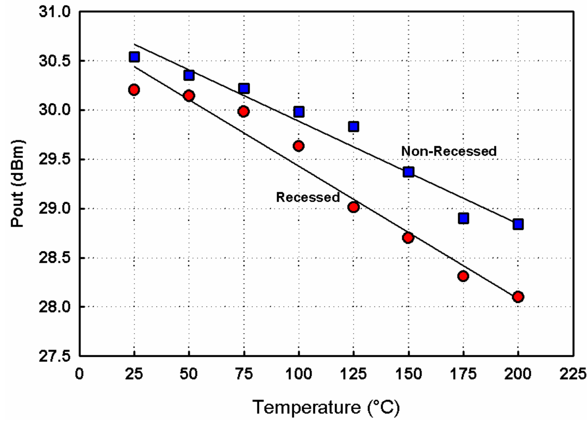

Fig. 6 Output power density at peak PAE as a function of temperature measured at 10 GHz of 300-µm recessed and non-recessed AlGaN/GaN HEMTs. $V_{DS} = 25$ V

The gate current remained constant over the temperature range under RF drive for the non-recessed devices, whereas the gate current decreased an order of magnitude for the non-recessed devices.

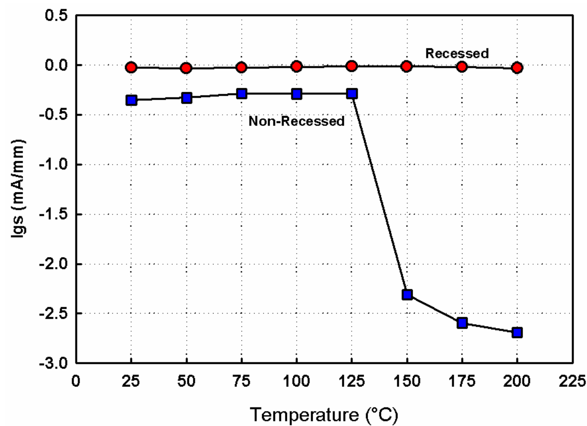

Fig. 7 The gate current at peak PAE as a function of temperature measured at 10 GHz of 300-µm recessed and non-recessed AlGaN/GaN HEMTs. $V_{DS} = 25$ V.

V. SUMMARY

In this paper, we have presented the DC, RF power, and high-temperature performance of recessed-gate AlGaN/GaN HEMTs. The devices have shown linear increase in power as a function of drain bias, minimal change in peak PAE, 2.5 – 3 dB increase in linear gain and associated gain. At high-temperature, the power density decreased at similar rate for both the recessed and non-recessed devices. More interestingly, the gate current under RF drive remained constant at -0.03 mA from 25 ° to 200 °C, which improved the associated gain at 200 °C by 3 dB compared with non-recessed devices.

ACKNOWLEDGEMENT

The authors would like to thank Shiping Guo from Emcore for epi material growth. We also thank G. Oliver for processing and L. Gooch for testing assistance at TriQuint.

REFERENCES

[1] Y. F. Wu, A. Sexler, M. Moore, R. P. Smith, S. Sheppard, P. M. Chavarkar, T. Wisleder, U. K. Mishra, and P Parikh, "30 W/mm GaN HEMTs by Field Plate Optimization," *IEEE Electron Device Lett.*, vol. 25, pp. 117 – 119, Mar. 2004.

[2] Y. Ando, Y. Okamoto, H. Miyamoto, T. Nakayama, T. Inoue, and M. Kuzuhara, "10 W/mm AlGaN-GaN HFET with a Field Modulating Plate," *IEEE Electron Device Lett.*, vol. 24, pp. 289-291, May 2003.

[3] Y. Okamoto, Y. Ando, K. Hataya, T. Nakayama, H. Miyamoto, T. Inoue, M. Senda, K. Hirata, M. Kosaki, N. Shibata, and M. Kuzuhara, "Improved Poer Performance for a Recessed-Gate AlGaN-GaN Heterojunction FET with a Field-Modulating Plate," *IEEE Trans. Microwave Theory and Tech.*, vol. 52, pp. 2536 – 2540, Nov. 2004.

[4] Y. Okamoto, Y. Ando, K. Hataya, T. Nakayama, H. Miyamoto, T. Inoue, M. Senda, K. Hirata, M. Kosaki, N. Shibata, and M. Kuzuhara,"179 W Recessed-Gate AlGaN/GaN Heterojunction FET with Field-Modulating Plate," *IEE Electronics Lett.*, vol. 40, pp. 629-631, May 2004.

[5] A. Chini, D. Buttari, R. Coffie, L. Shen, S. Heikman, A. Chakraborty, S. Keller, and U. K. Mishra, "Power and Linearity Characteristics of Field-Plated Recessed-Gate AlGaN-GaN HEMTs," *IEEE Electron Device Lett.*, vol. 25, pp. 229-231, May 2004.